CANCER GENOMICS & PROTEOMICS *15*: 485-497 (2018)
doi:10.21873/cgp.20107

NOTUM Is Involved in the Progression of Colorectal Cancer

JONG HYUK YOON[1*], DAYEA KIM[2*], JAEYOON KIM[3,4], HYEONGJOO LEE[4], JAEWANG GHIM[4], BYUNG JUN KANG[5], PARKYONG SONG[5], PANN-GHILL SUH[6], SUNG HO RYU[5] and TAEHOON G. LEE[4]

[1]*Department of Neural Development and Disease, Korea Brain Research Institute, Daegu, Republic of Korea;*
[2]*New Drug Development Center, Daegu-Gyeongbuk Medical Innovation Foundation, Daegu, Republic of Korea;*
[3]*School of Interdisciplinary Bioscience and Bioengineering and* [5]*Department of Life Sciences, Pohang University of Science and Technology (POSTECH), Pohang, Republic of Korea;*
[4]*NovaCell Technology, Inc., Pohang, Republic of Korea;*
[6]*School of Life Sciences, Ulsan National Institute of Science and Technology, Ulsan, Republic of Korea*

Abstract. *Background: There are limitations to current colorectal cancer (CRC)-specific diagnostic methods and therapies. Tumorigenesis proceeds because of interaction between cancer cells and various surrounding cells; discovering new molecular mediators through studies of the CRC secretome is a promising approach for the development of CRC diagnostics and therapies. Materials and Methods: A comparative secretomic analysis was performed using primary and metastatic human isogenic CRC cells. Proliferation was determined by MTT and thymidine incorporation assay, migration was determined by wound-healing assay (ELISA). The level of palmitoleoyl-protein carboxylesterase (NOTUM) in plasma from patients with CRC was determined by enzyme-linked immunosorbent assay. Results: NOTUM expression was increased in metastatic cells. Proliferation was suppressed by inhibiting expression of NOTUM. Knockdown of NOTUM genes inhibited proliferation as well as migration, with possible involvement of p38 and c-JUN N-terminal kinase in this process. The result was verified in patients with CRC. Conclusion: NOTUM may be a new candidate for diagnostics and therapy of CRC.*

*These Authors contributed equally to this work.

Correspondence to: Taehoon G. Lee, Ph.D., NovaCell technology, Inc., Pohang, Gyeongsangbuk-do, Republic of Korea. Tel: +82 542232475, Fax: +82 542232474, e-mail: taehoon@novacelltech.com; Jong Hyuk Yoon, Ph.D., Department of Neural Development and Disease, Korea Brain Research Institute, Daegu, South Korea. Tel: + 82 539808341, Fax: +82 539808399, e-mail: jhyoon@kbri.re.kr

Key Words: NOTUM, secretomics, colorectal cancer, migration, diagnosis.

Colorectal cancer (CRC) is the fourth most common malignancy and a leading cause of cancer-related mortality worldwide (1). Recent estimates suggest that the burden of CRC is expected to increase by 60% by 2030, with more than 2.2 million new cases and 1.1 million deaths (2). A large proportion of this burden could be prevented either by the screening and detection of this cancer at early stages when chances of a cure are substantially higher than at later stages, or by the detection and removal of precancerous lesions (3, 4). Nevertheless, primary screening faces limitations in terms of invasiveness, available capacities, costs, inconvenience, and adherence (5, 6). Although blood-based protein biomarkers such as carcinoembryonic antigen and carbohydrate antigen 19-9 are already utilized in the clinical setting, they cannot be used alone to screen or diagnose cancer because levels of these markers can be abnormal for reasons other than cancer, such as hepatitis and inflammatory bowel disease (7). Thus, there is an urgent need for new biomarkers and molecular targets with relatively high sensitivity and specificity to CRC.

Solid tumors such as CRC are composed of malignant cells along with other stromal cells such as neoplastic, mesenchymal, and inflammatory cells (8). Cancer cells interact with other cells through secreted factors, orchestrating complex signaling pathways (9). Cancer cells secrete various factors including soluble factors and proteases that alter adjacent stromal cells toward a permissive and supportive microenvironment for tumor progression (10). This cancer 'secretome' has been receiving increased interest for the discovery of diagnostic or prognostic cancer biomarkers, and can be a good tool for elucidating cancer biology (11, 12). Therefore, a comprehensive analysis of the cancer secretome can lead to discovery of potential biomarkers or therapeutic targets as well as give a microscopic insight into the cancer microenvironment.

SW480 and SW620 CRC cell lines were derived from primary and metastatic tumors, respectively, from the same

patient and have identical mutation profiles, but epigenetic differences (13). The monoclonal origin of these two cell lines was confirmed by the presence of shared marker chromosomes seen on cytogenetic analysis (14). Since variation due to genetic background can largely be disregarded for these two cell lines, they constitute a unique model for studying CRC progression and metastasis. Some studies have compared the two cell lines to find biomarkers using proteomic analysis (11, 15, 16). However, it is still necessary to study the secretome of these cells because of insufficient information regarding biomarkers or therapeutic targets.

Here, we performed a comparative secretomic analysis of conditioned medium from SW480 and SW620 cell cultures to characterize their CRC secretomes and to identify CRC-derived proteins and those associated with metastatic phenotype. The strategy for our research is outlined in Figure 1A.

Materials and Methods

Cell cultures. SW480 and SW620 CRC cell lines obtained from the ATCC (Manassas, VA, USA) were grown in Roswell Park Memorial Institute (RPMI) 1640 medium (Lonza Group, Basel, Switzerland) containing 10% fetal bovine serum and 1% penicillin/streptomycin (both from Gibco Life Technologies, Gaithersburg, MD USA) at 37˚C with 5% CO_2. Cells were monitored using a microscope (LSM 510 Meta; Ziess, Germany).

Preparation of conditioned medium. SW480 and SW620 cells were washed three times with phosphate-buffered saline (PBS). Conditioned medium was prepared by adding unsupplemented RPMI 1640 (no serum, phenol red, or antibiotics) to SW480 or SW620 cells, and incubating them for 24 h at 37˚C with 5% CO_2. Conditioned medium was then collected and centrifuged at 2,100 × *g* for 10 min (Combi-514R; Hanil Science Industry, Gimpo, Korea). After discarding of pellets, supernatants were collected for the next procedure.

Sample preparation for mass spectrometric (MS) analysis. The supernatants were filtered through Amicon Ultra-15 Centrifugal Filter Unit (UFC900324; Millipore, Tullagreen, Carrigtwohill Co. Cork, Ireland) for desalting and decontamination. The filtered supernatants were lyophilized. For tryptic digestion, dried samples were reduced using 10 mM dithiothreitol in 50 mM ammonium bicarbonate (ABC) and alkylated using 100 mM iodoacetamide in 50 mM ammonium bicarbonate. Finally, each sample was treated with trypsin (Promega, Madison, WI, USA) at a 1:50 ratio for 12 h at 37˚C and dried.

MS analysis. All MS analyses were carried out using a nano-liquid chromatography and MS system consisting of a high-performance liquid chromatography (HPLC) system (Agilent 1100; Agilent Technologies, Santa Clara, CA, USA) and a QSTAR quadrupole-TOF mass spectrometer (Applied Biosystems, Foster City, CA, USA; MDS SCIEX, Concord, ONT, Canada) equipped with a nano-electrospray ionization source. For high-resolution separation, a nanoscale RPC column (ZORBAX C18, 3 mm, 100 Å, 75 mm, i.d.; Agilent Technologies) was used. Mobile phase A consisted of HPLC-grade water containing 0.1% formic acid, and mobile phase B consisted of 84% HPLC-grade acetonitrile containing 0.1% formic acid. The separation was performed at a flow rate of 250 nl/min, and the applied gradient was 0-40% B over 60 min. For the tandem MS analysis, each scan cycle consisted of one full scan mass spectrum (m/z 400-1500) followed by three MS/MS events. Dynamic exclusion was activated for 1 min with a repeat count of 2. This study used three biological replicates for each condition in MS analyses.

Database search for identified secretome proteins. Analyst QS 2.0 (AB Sciex, Framingham, MA, USA) was used for data acquisition. Mascot Daemon version 2.2.2 (Matrix Science, Boston, MA, USA) generated mascot generic format files from the raw data files. The mascot generic format files were searched against the concatenated database consisting of sequences of *Homo sapiens* and *Bos taurus* from UniProt/Swiss-Prot (release 2018_03, EMBL-EBI), and their reverse sequences using MASCOT software version 2.2.04. The following search parameters were applied for database search: two missed cleavages were allowed; carbamidomethylation (C) as a fixed modification; pyroglutamylation (N-term EQ), oxidation (M), and *N*-acetyl (protein) as variable modifications; and +2, +3, and +4 charge ions were included. Peptide tolerance was 30 ppm and MS/MS tolerance was 0.5 Da. For peptide identification and protein assembly, MASCOT score=15 was used as the initial peptide filter, which estimated a 1% false discovery rate calculated using the target-decoy method (17). Proteins with no unique peptide or with only one spectral count were excluded identified. Proteins identified with a higher MASCOT score in the bovine database than that in the human database were also excluded from the list as they were considered as serum contaminants.

Quantitative analysis of MS results. In order to perform quantitative analysis of the identified proteins from two cell lines, the normalized spectral index based on the fragment ion intensity measurement was applied with modifications following a previous report (18). Briefly, the spectral index (SI) of each protein was calculated, which is the cumulative fragment ion intensity for identified peptides, and it was normalized (SI_N) by dividing the total sum of SI for all identified proteins (SI_T). To avoid taking logarithms for zero values, if no peptide was identified from a cell line, the spectral index was set as half the minimum value among all SI. The average SIN value from biological replicates in each group was acquired, and log2 ratio of normalized SI between the two groups, $\log_2(SI_{N\_A}/SI_{N\_B})$, was compared. For bioinformatic study, quantitatively analyzed proteins were analyzed through the use of Ingenuity Pathway Analysis (IPA; Ingenuity® Systems, www.ingenuity.com). Canonical pathways which were predicted to be influenced by the differentially expressed proteins were ranked in order of significance.

Tetrazolium (MTT) assay. SW480 and SW620 cells were cultured in a 96-well culture plate at a density of 3,000 cells/well. After 24 h, 10 μg/ml of palmitoleoyl-protein carboxylesterase (NOTUM) antibody (ab106448; Abcam, Cambridge, UK) and IgG antibody were added and cells were incubated for a further 72 h. After the medium was discarded, 0.5 mg/ml of MTT solution (Sigma-Aldrich, St. Louis, MO, USA) dissolved in serum-free medium was added and cells were incubated for 3 h at 37˚C in an atmosphere with 5% CO_2. The medium was then removed, and 100 μl of dimethyl sulfoxide was added to each well of the 96-well culture plate. The plate was vortexed for 10 min. Absorbance of the solution in each well was then measured at 540 nm using a Biotrak 2-plate reader (GE Healthcare, Chicago, IL, USA).

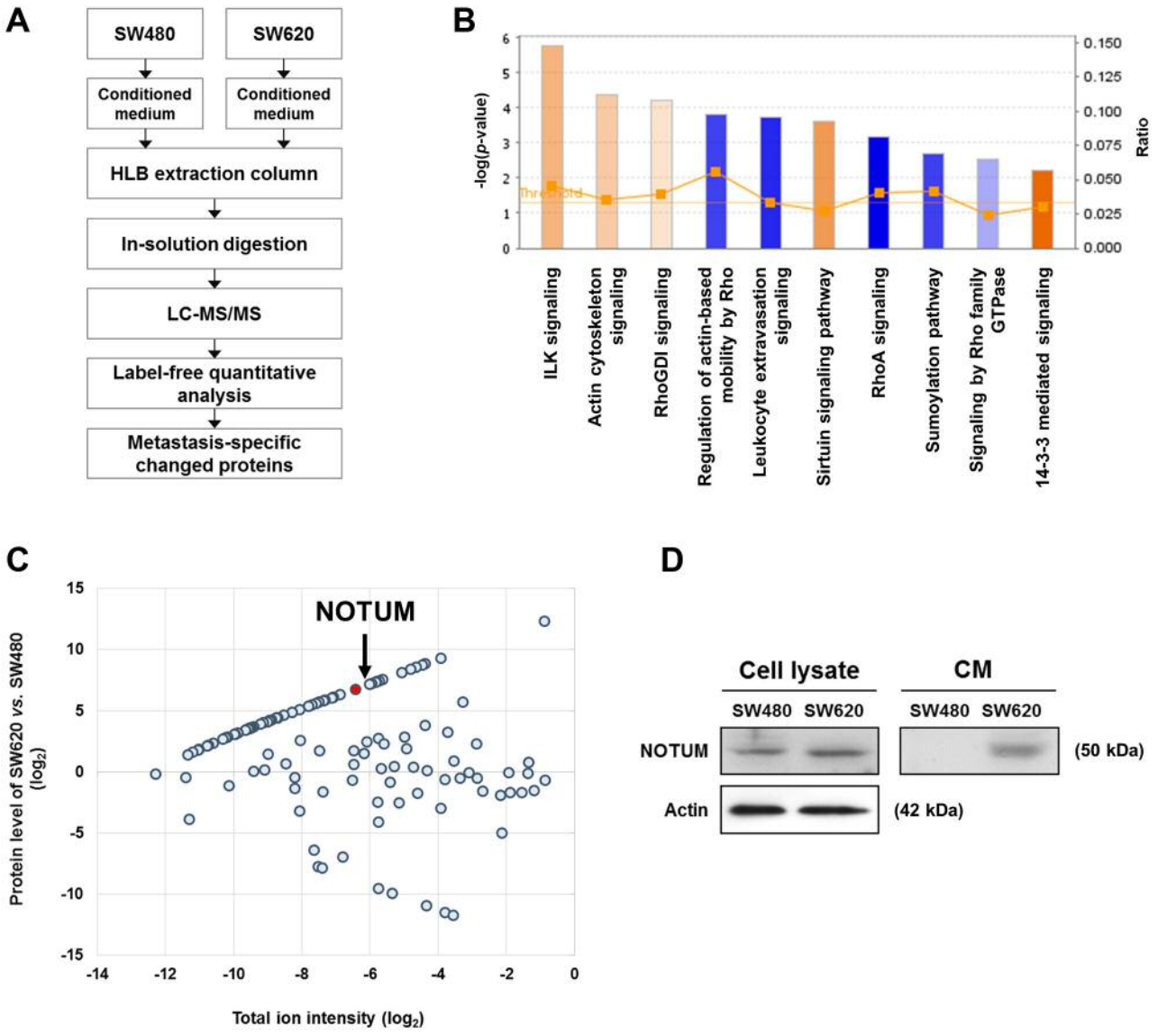

Figure 1. *Proteomic analysis of SW480 and SW620 colorectal cancer cell secretomes. A: Experimental strategy. B: Ingenuity Pathway Analysis of the identified proteins. Orange indicates a canonical pathway that was activated. Blue indicates a canonical pathway that was deactivated. Parameters for the analysis were z-score cut-off=0.5 and −log (p-value) >1.3. C: Virtual 2-D peptide map of SW620 vs. SW480 cells. The X-axis shows the total protein intensity, and the Y-axis shows the amount of individual proteins in SW620 vs. SW480 cell lines. Each dot indicates a secretory protein. The linear plot indicates the quantity of proteins in SW620 vs. those in SW480, where a protein level above 0 means more proteins secreted in SW620 than in SW480 cells. D: Immunoblot analysis for palmitoleoyl-protein carboxylesterase (NOTUM) in cell lysate and conditioned medium (CM).*

Thymidine incorporation assay. SW480 and SW620 cells were seeded in a 96-well culture plate at a density of 3,000 cells/well. After 24 h, anti-*NOTUM* small interfering RNA (siRNA) (GenePharma, Shanghai, China) and control siRNA (GenePharma) were added to the cells and plates were incubated for 4 h at 37˚C in an atmosphere with 5% CO_2. Sequences of siRNA used are given in Table I. The medium was changed to growth medium and plates were incubated for a further 72 h at 37˚C in an atmosphere with 5% CO_2. After incubation, cells were treated with ^{3}H-thymidine (0.3 mCi/0.3 ml, each well) in serum-free medium for 6 h then 0.2 ml of 10% trichloroacetic acid was added and plates were incubated at 4˚C for 30 min; 1 M NaOH was added to the plates which were incubated at 3˚C for 25 min. Radioactivity in DNA was measured by scintillation counter (Perkin Elmer, Waltham, MA, USA).

Wound-healing assay. SW480 and SW620 cells were seeded in a 6-well culture plate at a density of 1.5×10^5 cells/well. After 12 h, *NOTUM* siRNA and scrambled siRNA were added and plates were

Table I. *List of small interfering RNA (siRNA) sequences used in this study.*

siRNA name		Sequence	
		Sense (5'-3')	Antisense (5'-3')
Control		UUCUCCGAACGUGUCACGUTT	ACGUGACACGUUCGGAGAATT
NOTUM	#1	AGTCTGAGAAGAACGAGTA	TACTCGTTCT TCTCAGACT
	#2	CCCTACTGGTGGAACGCAA	TTGCGTTCCA CCAGTAGGG
	#3	GGACAGCTTCATGGCGCAA	TTGCGCCATG AAGCTGTCC

incubated for another 72 h. A wound was made by scratching in the central area of the plates with a pipette tip, and the detached cells were gently washed out. Cell migration was observed at 1, 12, 24, 36, and 48 h after scratching. Images were taken of each wounded area under light microscopy.

Immunoblotting. Untreated cells were washed with 1× PBS and lysed with lysis buffer (150 mM NaCl, 10 mM Tris-HCl, pH 7.4, 1% Triton X-100, 1 mM ethylenediaminetetra-acetic acid 0.5% phenylmethylsulfonyl fluoride and 0.5% protease inhibitor). Human blood plasma was also lysed with the lysis buffer. Protein concentrations were measured by Bradford assay. Proteins (10 μg in each lane) were electrophoresed on 6-16% or 6-20% sodium dodecyl sulphate–polyacrylamide gels then transferred onto nitrocellulose membrane using the Hoefer wet transfer system. The membranes were blocked by tris buffered saline with tween 20 (TBS-T) buffer containing 5% skimmed milk for 30 min and incubated for 18 h at 4˚C with primary antibodies against NOTUM (Abcam), p110α (Cell Signaling Technology), phosphorylated protein kinase B (pAKT) Ser473 Cell Signaling Technology), pAKT Thr308 (Cell Signaling Technology), AKT1/2 (Santa Cruz), phosphorylated extracellular-signal-regulated kinase (pERK) 1/2 Cell Signaling Technology), ERK1/2 (Cell Signaling Technology), cyclin D1 (Cell Signaling Technology), p-p38 (Thermo Fisher), p38 (Thermo Fisher), c-JUN *N*-terminal kinase1/2 (JNK1/2) (Cell Signaling Technology), p-JNK1/2 (Cell Signaling Technology), β-actin (MP Biomedicals), and glyceraldehyde-3-phosphate dehydrogenase (GAPDH) (Cell Signaling Technology). After incubation, membranes were washed six times with TBS-T. The blots were incubated with horseradish peroxidase-conjugated anti-mouse, anti-rabbit (SeraCare, Milford, MA, USA), and anti-goat antibody (Santa Cruz, Dallas, TX, USA) for 2 h at room temperature with mild rotation. The membranes were washed with TBS-T six times and then developed by using electrochemiluminescence (ECL) solution (GE Healthcare). Western blot results were densitometrically analyzed using ImageJ (ver. 1.51).

Human tissue samples. Human blood plasma from healthy controls and patients with CRC were randomly selected by the National Cancer Center (South Korea). Participants provided informed consent, and protocols were approved by the Institutional Review Board of National Cancer Center (South Korea) (NCCCTS08351). All groups consisted of 42-to 77-year-olds without significant sex difference. Three healthy samples from controls (42 to 67 years old, two males, one female), three from patients with stage I (61 to 77 years old, males), seven with stage II (43 to 76 years old, four males, two females), nine with stage III (42 to 68 years old, six males, three females), and one with stage IV (63 years old, female) CRC samples were used. All plasma was collected by fine-needle aspiration during pre-operative blood draw and collected in tubes with heparin. All plasma was shipped within 1 day of collection, packed with dry ice and stored at −80˚C before analysis of NOTUM concentration.

ELISA. Plasma specimens were diluted 1/10 with 100 mM bicarbonate/carbonate buffer and coated onto a 96-well plate for 24 h at 4˚C. The plates were washed three times with PBS and blocked with 5% skimmed milk/PBS for 24 h at 4˚C. The plates were washed three times and incubated with primary antibody (ab106448; Abcam) for 2 h at room temperature. Next the plates were washed three times with 0.05% Tween-20 and incubated with horseradish peroxidase-conjugated goat anti-rabbit IgG secondary antibody for 2 h at room temperature. After three times washing with PBS, 100 μl of ultra tetramethyl benzidine solution was added to each well and incubated for 20 min at room temperature. Sulfuric acid (2 M) was treated to stop the reaction, and the absorbance was then measured at 450 nm. Absorbance normalized by total protein amount was used as the absorbance index.

Statistical analysis. For the secretome study, proteins identified as differentially secreted between the two CRC cell lines were those with *t*-test $p<0.05$ obtained using an integrative statistical hypothesis testing, which combines F-tests obtained from two-tailed Student's *t*-test. Significance of proliferation and wound-healing assays was evaluated by two-tailed Student's *t*-test; differences with $p<0.05$ were considered statistically significant.

Results

Comparative proteomic analysis of SW480 and SW620 CRC cell lines. To compare the secretory protein profile of SW480 and SW620 CRC cell lines, we applied reliable label-free quantitative proteomics analysis. We identified 124 proteins from SW480 and SW620 cells in total. The list of representative proteins of which the levels differed significantly between the two cell lines is shown in Table II. To identify the biological features of the identified proteins, IPA was used. We directly applied the quantitative proteomic result to IPA. Five out of 10 canonical pathways were activated in the secretome of SW620 (z-score cutoff=0.1, −log (*p*-value) >1.3) (Figure 1B). Integrin linked

kinase (ILK), actin cytoskeleton, RhoGDI, sirtuin, and 14-3-3-mediated signaling were activated, while actin-based mobility by Rho, leukocyte extravasation, RhoA, sumoylation, and Rho family GTPase signaling were deactivated in the secretome of SW620 (Figure 1B). This indicates that the canonical pathways involved in metastatic features of CRC (19) were changed. We plotted a virtual 2-D protein map by using the fold change of protein expression in SW480 and SW620 against the total ion intensity (Figure 1C). We found a series of plots that showed an increase or decrease proportional to the increase or decrease of total ion intensity. This indicated reliability of the quantitative proteomic results.

We used three criteria to screen proteins for further study, namely whether the protein was increased in the secretome of SW620 cells compared with SW480 cells, whether it had signaling sequences, and whether its involvement in cancer progression was unknown (20-23). We selected NOTUM whose level was clearly increased in the secretome of SW620 cells ($\log_2$R=6.78). We verified this increase by immunoblotting (Figure 1D). NOTUM is an extracellular enzyme induced by high levels of Wingless activity in *Drosophila* (24). It is anchored to the cell surface by binding to glypican-like sulfated proteoglycans, and it functions as a glypican-dependent Wnt inhibitor (25). NOTUM regulates head formation and neural induction in *Xenopus* (26), and activity of hedgehog proteins in *Drosophila* (27). Recently, its overexpression in some human hepatocellular carcinomas and CRCs has been reported (28, 29). We first verified intracellular and extracellular protein levels of NOTUM in CRC cell lines. The NOTUM level was found to be slightly increased in SW620 compared to SW480 in the whole cell lysate. However, the level of NOTUM was drastically increased in the conditioned medium of SW620 metastatic CRC cells (Figure 1D).

Secreted NOTUM affected proliferation of CRC cells. We hypothesized that the secreted NOTUM had a regulatory function in cancer progression because NOTUM was secreted by SW620 cells as shown in Figure 1D. We checked whether the neutralization of secreted NOTUM affected the proliferation of CRC cells. After treatment of both SW480 and SW620 cell lines with anti-NOTUM for 72 h, the proliferative activities of SW480 and SW620 cells were found to be significantly reduced (Figure 2). Furthermore, the reductive effect was greater in SW620 than in SW480 cells. This indicates that secreted NOTUM has a role in CRC progression, and its effect is stronger in metastatic than in primary CRC cells.

Involvement of NOTUM in proliferation and migration of CRC cells. We performed knockdown of NOTUM gene in SW480 and SW620 calls using siRNAs. The efficacy of knockdown is shown in Figure 3. Knockdown of *NOTUM* clearly reduced proliferative activity as measured by thymidine incorporation assay compared to the control, regardless of cell type (Figure 4A). Next, the migratory activity was determined using wound-healing assay after the knockdown of *NOTUM*. Migration of SW480 cells was assessed every 12 h and was found to be reduced from 12 h up to 48 h, with statistical significance (Figure 4B). We also found that the reduction of migration SW620 cells was similar to that of SW480 cells (Figure 4C).

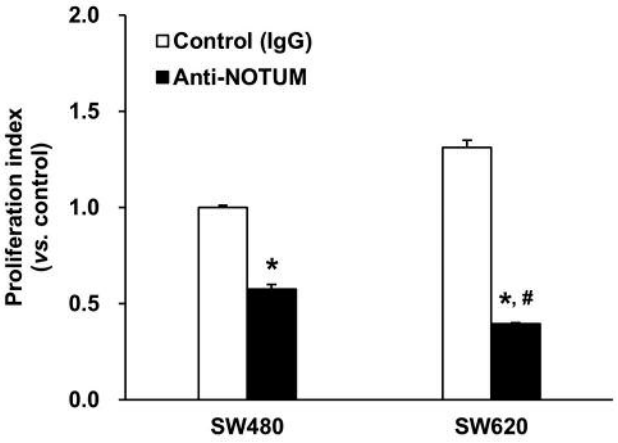

Figure 2. *Proliferation of SW480 and SW620 colorectal cancer cells under palmitoleoyl-protein carboxylesterase (NOTUM) neutralization. Tetrazolium (MTT) assay for proliferation was performed in the presence of 400 nM antibody to NOTUM or control IgG. Data are shown as the mean±standard error of the mean. Significantly different at: *p<0.05 versus control IgG (two-tailed Student's t-test); #p<0.05 against control IgG of SW480 (two-tailed Student's t-test).*

Up-regulation of p38 and JNK pathways due to NOTUM knockdown in CRC cells. It has been reported that stimulating AKT or mitogen-activated protein kinase (MAPK) pathways regulated CRC progression (30, 31). To understand the underlying mechanisms responsible for cell proliferation and migration induced by NOTUM in CRC, cells were treated with *NOTUM* siRNA or control siRNA and expression of AKT-, ERK-, p38-, and JNK-related signal molecules was analyzed. Firstly, we examined AKT signaling, which is generally known as a proliferative pathway in various cell types (32, 33). AKT-related signaling components including phosphatidylinositol 3-kinase (PI3KCA) catalytic subunit (p110α), p-AKT, and AKT1/2 were not affected by *NOTUM* knockdown (Figure 5A). Expression of proteins of the ERK signaling pathway, p-ERK1/2, ERK1/2, and its downstream molecule cyclin D1 did not change (Figure 5B). On the other hand,

Table II. *List of representative proteins changed in conditioned media of SW480 and SW620 (log_2>2).*

Accession	Name	Coverage (%)	Mascot score	Unique peptides	Log_2R	*p*-Value
Q07654	Trefoil factor 3	91.5	2722.91	60	12.32	<0.001
P36955	Pigment epithelium-derived factor	32.1	4211.06	76	9.28	0.002
P12830	Cadherin-1	4.4	1390.4	24	8.83	<0.001
P05787	Keratin, type II cytoskeletal 8	30	2638.85	52	8.74	0.025
P61769	Beta-2-microglobulin	30.6	1747.46	36	8.56	0.002
Q99574	Neuroserpin	29.4	3166.09	48	8.40	0.004
P00558	Phosphoglycerate kinase 1	39.4	2182.86	43	8.13	0.004
P19338	Nucleolin	4.5	672.16	14	7.56	0.006
P98160	Basement membrane-specific heparan sulfate proteoglycan core protein	6.1	2812.95	75	7.47	0.037
P24821	Tenascin	3.8	1740.31	27	7.38	0.007
P19021	Peptidyl-glycine alpha-amidating monooxygenase	5	979.97	22	7.36	0.004
P07900	Heat-shock protein (HSP 90-alpha)	18.6	1094.84	27	7.25	0.010
P14543	Nidogen-1	4.7	433.04	8	7.18	0.118
Q6P988	Palmitoleoyl-protein carboxylesterase (NOTUM)	6.9	1133.46	18	6.76	0.008
Q13740	CD166 antigen	2.5	353.83	8	6.31	0.053
O94985	Calsyntenin-1	5.6	772.96	16	6.11	0.046
P25311	Zinc-alpha-2-glycoprotein	25.9	558.73	12	6.10	0.022
O94808	Glutamine--fructose-6-phosphate aminotransferase (isomerizing) 2	1.3	229.29	9	6.06	0.120
Q5T2S8	Armadillo repeat-containing protein 4	0.6	377.53	9	5.85	0.010
Q9GZX9	Twisted gastrulation protein homolog 1	7.6	457.59	9	5.81	<0.001
P01033	Metalloproteinase inhibitor 1	59.2	4303.88	87	5.72	0.001
P04156	Major prion protein	5.8	478.9	9	5.68	0.251
P17096	High mobility group protein HMG-I/HMG-Y	23.6	169.18	4	5.60	0.354
Q92520	Protein FAM3C	6.4	393.52	7	5.47	0.001
P05783	Keratin, type I cytoskeletal 18	13.5	685.88	22	5.36	0.011
P23284	Peptidyl-prolyl cis-trans isomerase B	11.5	90.98	4	5.36	0.122
P11021	Endoplasmic reticulum chaperone BiP	4.2	239.05	4	5.11	0.172
P13639	Elongation factor 2	4.1	418.08	7	4.88	0.062
Q13308	Inactive tyrosine-protein kinase 7	3	444.71	8	4.88	0.016
P10599	Thioredoxin	19.2	196.13	6	4.63	0.091
Q3ZBD7	Glucose-6-phosphate isomerase	4.9	120.99	5	4.43	0.308
P30101	Protein disulfide-isomerase A3	2.5	172.61	4	4.42	0.207
P09341	Growth-regulated alpha protein	27.9	273.07	7	4.41	0.195
P23142	Fibulin-1	8.3	275.82	5	4.40	0.127
O00299	Chloride intracellular channel protein 1	7.5	216.28	3	4.23	0.176
Q01469	Fatty acid-binding protein, epidermal	20.1	245.73	8	4.19	<0.001
P81605	Dermcidin	15.4	147.39	3	4.18	0.392
P52799	Ephrin-B2	4.9	73.97	2	4.11	0.173
P09493	Tropomyosin alpha-1 chain	12.3	110.48	3	4.00	0.395
P20962	Parathymosin	16.8	489.45	11	3.91	0.332
P11142	Heat-shock cognate 71 kDa protein	21.2	2779.18	57	3.80	0.033
P35579	Myosin-9	0.8	542.21	6	3.70	0.014
Q14974	Importin subunit beta-1	1	88.83	3	3.62	0.256
P50395	Rab GDP dissociation inhibitor beta	7.4	146.11	4	3.60	0.144
P51888	Prolargin	2.5	83.11	4	3.56	0.002
P23526	Adenosylhomocysteinase	3.2	65.55	2	3.56	0.138
P16949	Stathmin	8.8	120.01	2	3.54	0.141
Q8NC51	Plasminogen activator inhibitor 1 RNA-binding protein	2	241.36	9	3.50	0.021
Q15582	Transforming growth factor-beta-induced protein ig-h3	3.6	214.87	5	3.43	0.205
P52209	6-Phosphogluconate dehydrogenase, decarboxylating	3.5	100.62	3	3.43	0.407
P02769	Serum albumin	42.4	4459.07	97	3.23	0.065
P08727	Keratin, type I cytoskeletal 19	9.8	174.2	2	3.18	0.283
O60568	Procollagen-lysine,2-oxoglutarate 5-dioxygenase 3	2.2	79.45	2	3.10	0.147
P21926	CD9 antigen	10.6	128.69	3	3.08	0.223
P10145	Interleukin-8	47.8	62.38	2	3.08	0.372
P22692	Insulin-like growth factor-binding protein 4	16	1275.9	12	2.85	0.079
P31946	14-3-3 protein beta/alpha	9.8	140.46	5	2.84	0.220

Table II. *Continued*

Table II. *Continued*

Accession	Name	Coverage (%)	Mascot score	Unique peptides	Log_2R	*p*-Value
P43243	Matrin-3	2.1	67.86	2	2.78	0.163
Q05716	Insulin-like growth factor-binding protein 4	9.3	757.1	15	2.71	0.001
Q9Y6N7	Roundabout homolog 1	1.5	289.91	9	2.69	0.249
P55001	Microfibrillar-associated protein 2	12.7	351.74	8	2.57	0.091
P68133	Actin, alpha skeletal muscle	9.9	1260.71	28	2.48	0.002
Q9H1U9	Solute carrier family 25 member 51	2.4	158.84	2	2.35	0.223
P40926	Malate dehydrogenase, mitochondrial	17.8	805.35	10	2.31	0.127
P05067	Amyloid-beta A4 protein	28.9	5973.29	111	2.29	0.007
Q9BRK5	45 kDa calcium-binding protein	3.1	92.67	3	2.17	0.193
Q13421	Mesothelin	8.4	85.51	3	2.12	0.302
P06748	Nucleophosmin	10.9	1151.78	24	−2.49	0.046
P09382	Galectin-1	13.4	1339.73	22	−2.51	0.001
P07355	Annexin A2	7.7	1433.65	32	−2.99	0.066
P24534	Elongation factor 1-beta	10.7	122.9	4	−3.20	0.155
Q8NBJ4	Golgi membrane protein 1	2.7	48.6	2	−3.90	0.262
P18065	Insulin-like growth factor-binding protein 2	24.8	845.48	16	−4.11	0.104
P00441	Superoxide dismutase (Cu-Zn)	69.9	4403.06	97	−4.99	0.002
P68104	Elongation factor 1-alpha 1	10	203.27	5	−6.41	0.173
P61604	10 kDa heat shock protein, mitochondrial	26.7	154.55	4	−6.96	0.169
P10909	Clusterin	6.3	184.5	3	−7.76	0.018
Q99435	Protein kinase C-binding protein NELL2	9.3	234.53	6	−7.88	0.121
Q86TH1	ADAMTS-like protein 2	4.4	229.28	5	−9.54	0.117
P16070	CD44 antigen	4.7	1193.63	23	−9.94	0.001
Q9UBT3	Dickkopf-related protein 4	15	1733.23	41	−10.94	0.006
P01037	Cystatin-SN	46.3	1075.85	25	−11.50	0.009
Q16270	Insulin-like growth factor-binding protein 7	23.8	449.39	9	−11.74	<0.001

although the levels of p38 and JNK1/2 were not affected by *NOTUM* knockdown (Figure 6A), phosphorylated p38, and JNK1/2 levels under *NOTUM* knockdown increased compared to the control (Figure 6A and B). In addition, the levels of p-JNK1 and p-p38 were higher in SW620 than those in SW480 cells (Figure 6A and B). These data indicate that NOTUM induced cell proliferation and migration *via* JNK and p38 MAPK inhibition, especially in metastatic CRC cells.

Increase in plasma NOTUM level in patients with CRC. We finally tried to verify reliability and applicability of NOTUM in diagnostics and treatment of patients with CRC. Twenty-three blood specimens from groups of healthy controls and stage-divided CRC patients. Using ELISA, we found a clear increase in absorbance in plasma of patients with CRC compared to the healthy controls (Figure 7A). This observation indicates reliability of our results and suggests NOTUM to be a potential biomarker of CRC. The plasma NOTUM level was the highest in patients with stage I CRC (Figure 7B). We also performed immunoblotting for NOTUM in plasma and found that the plasma NOTUM level was higher in patients with CRC (Figure 8).

Discussion

We profiled 124 proteins from the secretome of isogenic primary and metastatic CRC cells using reliable label-free quantitative proteomic analysis. Providing fundamental data for elucidation of CRC, we identified NOTUM as a candidate CRC-specific biomarker and therapeutic target. Based on our experimental results, NOTUM was associated with proliferation and migration of CRC cells and we the regulation of phosphorylation of p38 and JNK. The NOTUM level was elevated in plasma of patients with CRC (Figure 7). This result suggests the high potential of NOTUM to be developed as a biomarker and therapeutic target for CRC.

NOTUM is a 56-kDa evolutionarily-conserved secreted deacylase that regulates Wnt signaling activity (26). Earlier studies have shown that NOTUM regulates development in *Drosophila*, while its function in mammals was only recently characterized (25). NOTUM is overexpressed in hepatocellular carcinoma (28) and is also related to gastric cancer (34). These observations suggest that NOTUM has a role in other cancer types but do not provide any association between NOTUM and CRC. A recently published report demonstrated that the NOTUM level in colon mucosae was enhanced in a mouse

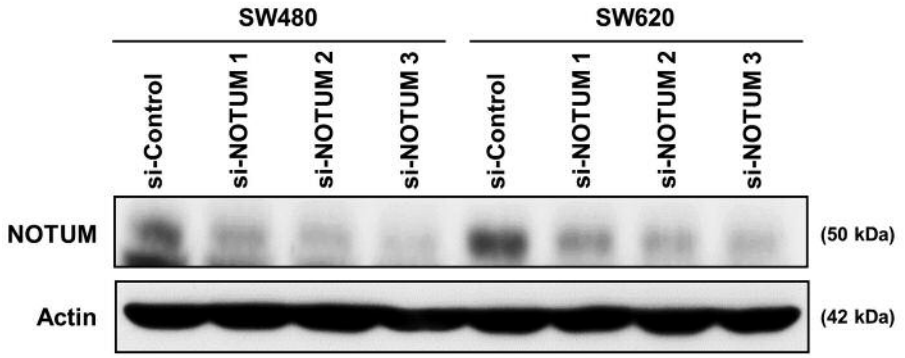

Figure 3. *Efficacy of palmitoleoyl-protein carboxylesterase (NOTUM) knockdown. Immunoblot analysis for NOTUM knockdown efficiency after small interfering RNA (siRNA) treatment. NOTUM knockdown efficacy was 30-40%.*

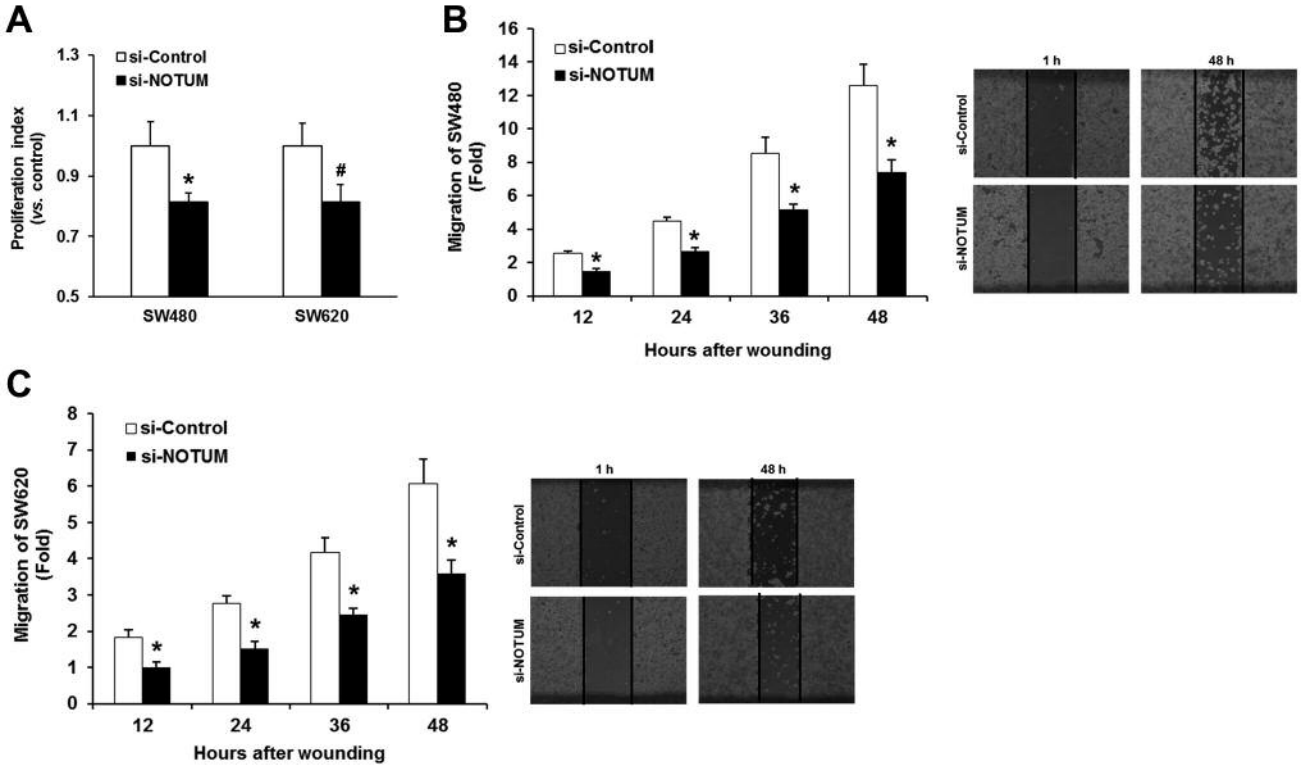

Figure 4. *Proliferation and migration assays after palmitoleoyl-protein carboxylesterase (NOTUM) knockdown SW480 and SW620 colorectal cancer cells. A: Thymidine incorporation assay for the measurement of proliferation of control or NOTUM siRNA-transfected cells. Wound-healing assay for measurement of migration of SW480 (B) and SW620 (C) cells under NOTUM knockdown. After treatment with small interfering RNA (siRNA), the cell layer was scratched with a sterile pipette tip, and measurement of migrated cells was performed at 12, 24, 36, and 48 h. Images were taken using a 4× objective. Data are shown as the mean±standard error of the mean, n=5. *Significantly different at p<0.05 compared with the control; #p=0.06.*

model of CRC (29). In line with this observation, we found that the NOTUM level increased in the secretome of human metastatic CRC cells. Moreover, NOTUM was found to be required for proliferation and migration of CRC cells regardless of their aggressiveness (Figure 4). Because two phenotypes such as proliferation and migration are difficult to completely distinguish in cancer, further study is needed to determine whether NOTUM changes the Rho GTPase

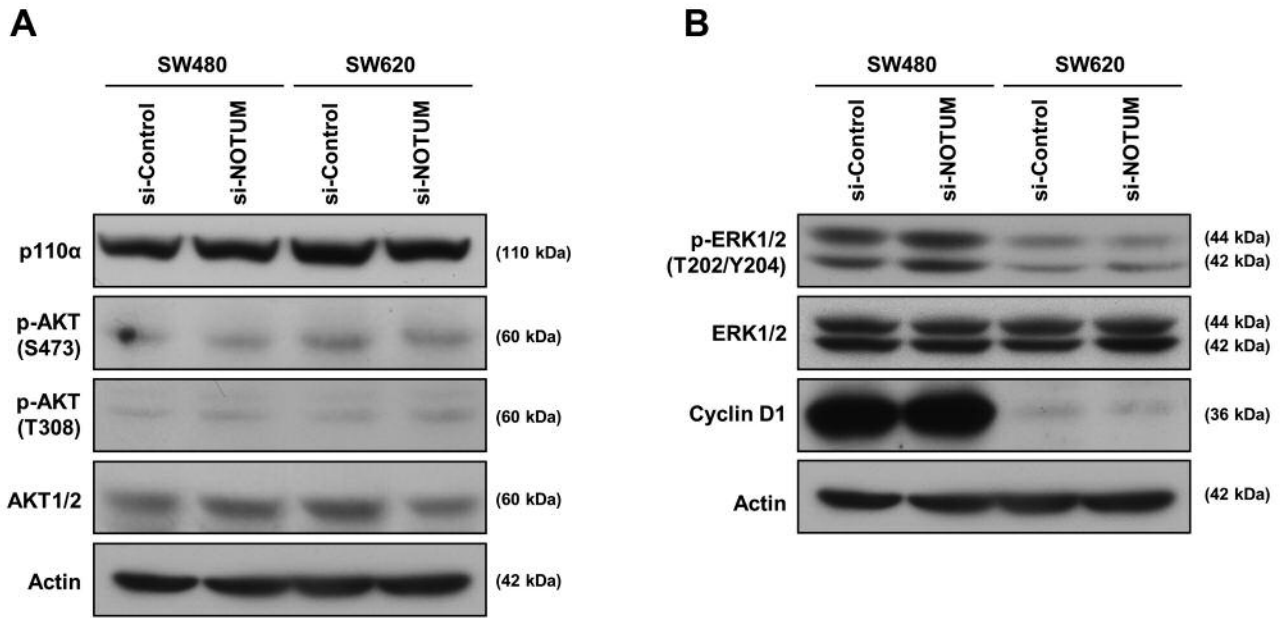

Figure 5. *Immunoblotting of proteins of signal pathways after palmitoleoyl-protein carboxylesterase (NOTUM) knockdown in SW480 and SW620 colorectal cancer cells. Immunoblot analysis of p110α, phosphorylated protein kinase B (p-AKT), and AKT1/2 (A), phosphorylated extracellular-signal-regulated kinase 1/2 (p-ERK1/2), ERK1/2 and cyclin D1 (B) in SW480 and SW620 cells after NOTUM knockdown. β-Actin was used as a loading control.*

signaling pathway and cell morphology appropriate for migration to confirm NOTUM increases cell migration. Taken together we suggest the possibility that NOTUM is a new biomarker as well as therapeutic target of CRC.

NOTUM was increased in plasma of patients with early-stage CRC rather than in late-stage (Figure 7). Because we observed this phenomenon using two proven experimental methods, we conclude that NOTUM can be used for diagnosis of early-stage CRC. It is known that colon cancer can be initiated and grow through the colon wall without metastasis at an early stage. When we consider lymph node or distant metastasis was observed from patients with stage III CRC at which the prognosis rapidly deteriorated (35, 36), we hypothesize that the potential role of NOTUM in CRC would be to initiate or support cancer cell growth to proceed to late stage disease. Once these cells have acquired vigorous metastatic characteristics, NOTUM would no longer be required for cancer progression.

In our study, phosphorylation of JNK and p38 was up-regulated under NOTUM knockdown (Figure 6). NOTUM cleaves members of the glypican family related to Wnt, Hedgehog, transforming growth factor β (TGF-β), and bone morphogenetic protein signaling (25, 37, 38). Because glypicans maintain secreted signaling molecules at the cell surface to activate high-affinity signaling receptors and ensure activation of target genes, NOTUM, as a lipase, can act as a negative regulator of growth factors (39-42). It has been reported that TGF-β suppresses tumorigenesis (43-46). The involvement of the p38 MAPK pathway in cell survival is well established (47-49). p38α negatively regulates cell-cycle progression and induces apoptosis (50). Moreover, mice with liver-specific deletion of p38α developed more liver tumors (50). Another report showed that p38α activity was down-regulated in human hepatocellular carcinoma (51). Regarding JNK, although there is increasing evidence of JNK-mediated apoptosis (52, 53), its involvement in cancer remains unresolved. On the other hand, mothers against decapentaplegic homolog 7 (SMAD7) and transforming growth factor B-activated kinase 1 (TAK1) induce apoptosis *via* the TGF-β pathway through p38 and JNK activation (54). Recently, a report showed that JNK and p38 MAPK pathways are also related to CRC (55). We suggest the possibility that NOTUM inhibition may induce TGF-β-mediated p38 and JNK signaling, and suppress cell proliferation and migration, although mechanistic studies are required to elucidate this.

Acknowledgements

The Authors thank the National Cancer Center (Republic of Korea) that provided blood plasma samples. This research was supported by GRL Program (NRF-2016K1A1A2912722) and by KBRI basic research program (18-BR-02-01), funded by Ministry of Science

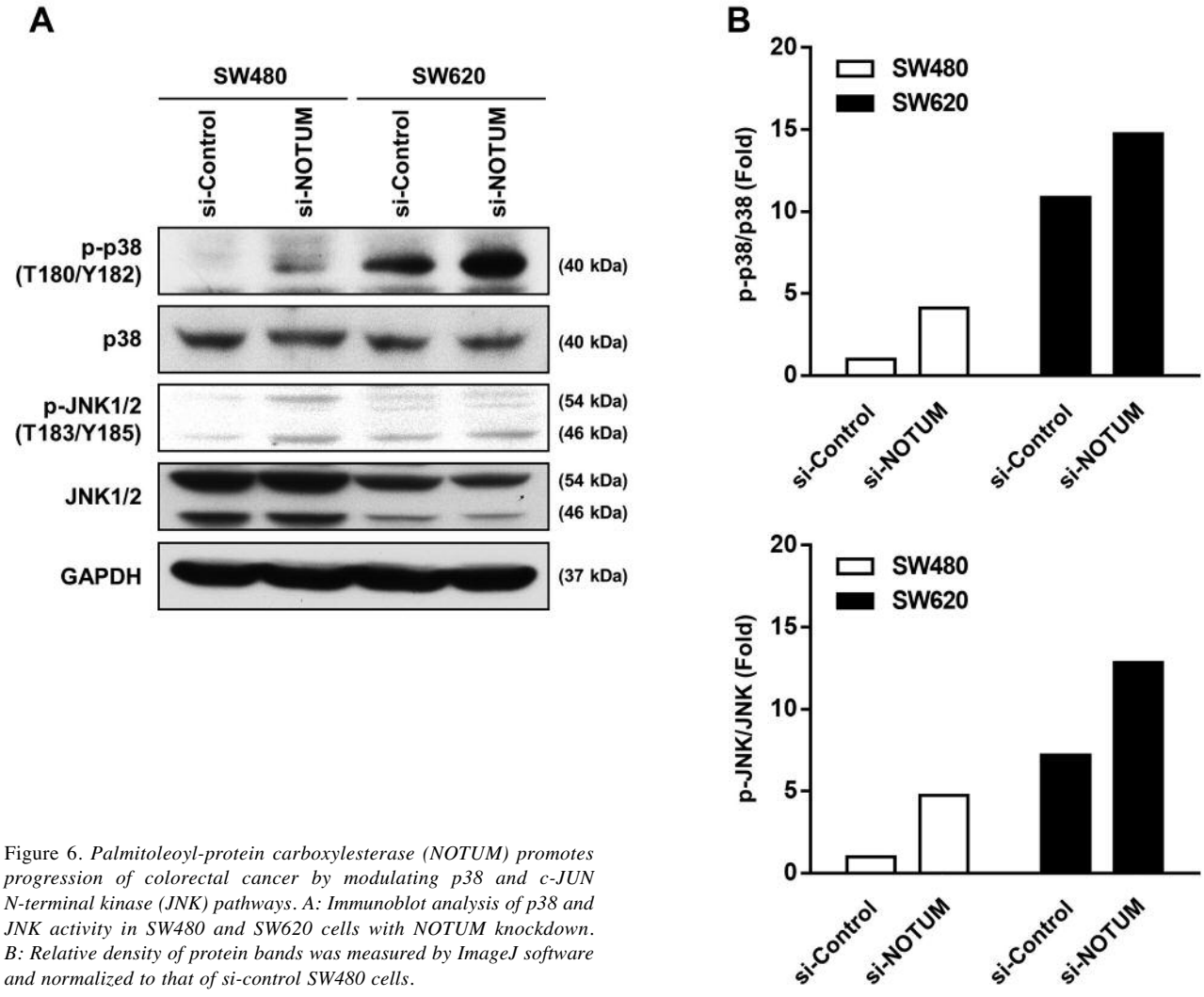

Figure 6. *Palmitoleoyl-protein carboxylesterase (NOTUM) promotes progression of colorectal cancer by modulating p38 and c-JUN N-terminal kinase (JNK) pathways. A: Immunoblot analysis of p38 and JNK activity in SW480 and SW620 cells with NOTUM knockdown. B: Relative density of protein bands was measured by ImageJ software and normalized to that of si-control SW480 cells.*

and ICT. This research was supported by Basic Science Research Program through the National Research Foundation of Korea funded by the Ministry of Education (2018R1D1A1B07043929). This research was also supported by grants from the National Cancer Center, Republic of Korea (NCC 1810861-1).

References

1 Ferlay J, Soerjomataram I, Dikshit R, Eser S, Mathers C, Rebelo M, Parkin DM, Forman D and Bray F: Cancer incidence and mortality worldwide: Sources, methods and major patterns in GLOBOCAN 2012. Int J Cancer *136(5)*: E359-386, 2015.

2 Arnold M, Sierra MS, Laversanne M, Soerjomataram I, Jemal A and Bray F: Global patterns and trends in colorectal cancer incidence and mortality. Gut *66(4)*: 683-691, 2017.

3 Brenner H, Stock C and Hoffmeister M: Effect of screening sigmoidoscopy and screening colonoscopy on colorectal cancer incidence and mortality: Systematic review and meta-analysis of randomised controlled trials and observational studies. BMJ *348*: g2467, 2014.

4 Zauber AG: The impact of screening on colorectal cancer mortality and incidence: Has it really made a difference? Dig Dis Sci *60(3)*: 681-691, 2015.

5 Lansdorp-Vogelaar I, Knudsen AB and Brenner H: Cost-effectiveness of colorectal cancer screening. Epidemiol Rev *33*: 88-100, 2011.

6 Hassan C, Giorgi Rossi P, Camilloni L, Rex DK, Jimenez-Cendales B, Ferroni E, Borgia P, Zullo A, Guasticchi G and Group HTA: Meta-analysis: Adherence to colorectal cancer screening and the detection rate for advanced neoplasia, according to the type of screening test. Aliment Pharmacol Ther *36(10)*: 929-940, 2012.

7 van der Schouw YT, Verbeek AL, Wobbes T, Segers MF and Thomas CM: Comparison of four serum tumour markers in the diagnosis of colorectal carcinoma. Br J Cancer *66(1)*: 148-154, 1992.

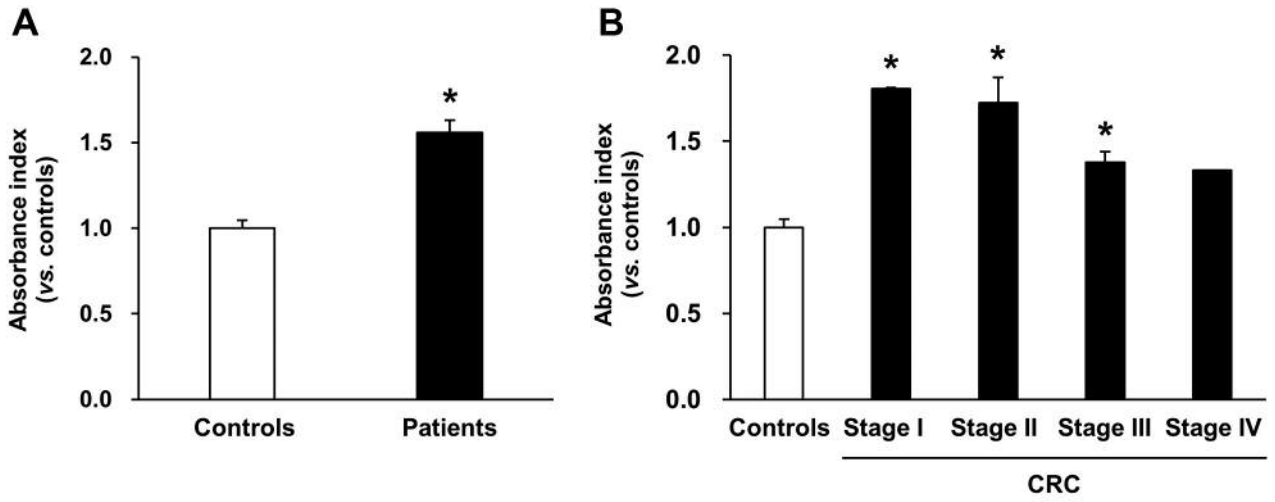

Figure 7. *Plasma palmitoleoyl-protein carboxylesterase (NOTUM) levels, as determined by enzyme-linked immunosorbent assay in patients with colorectal cancer (CRC) and healthy individuals. A: Plasma NOTUM levels for healthy and CRC patient groups. B: Plasma NOTUM levels for healthy and patient groups according to CRC stage. Data are shown as the mean±standard error of the mean. *Significantly different at p<0.05 versus healthy controls.*

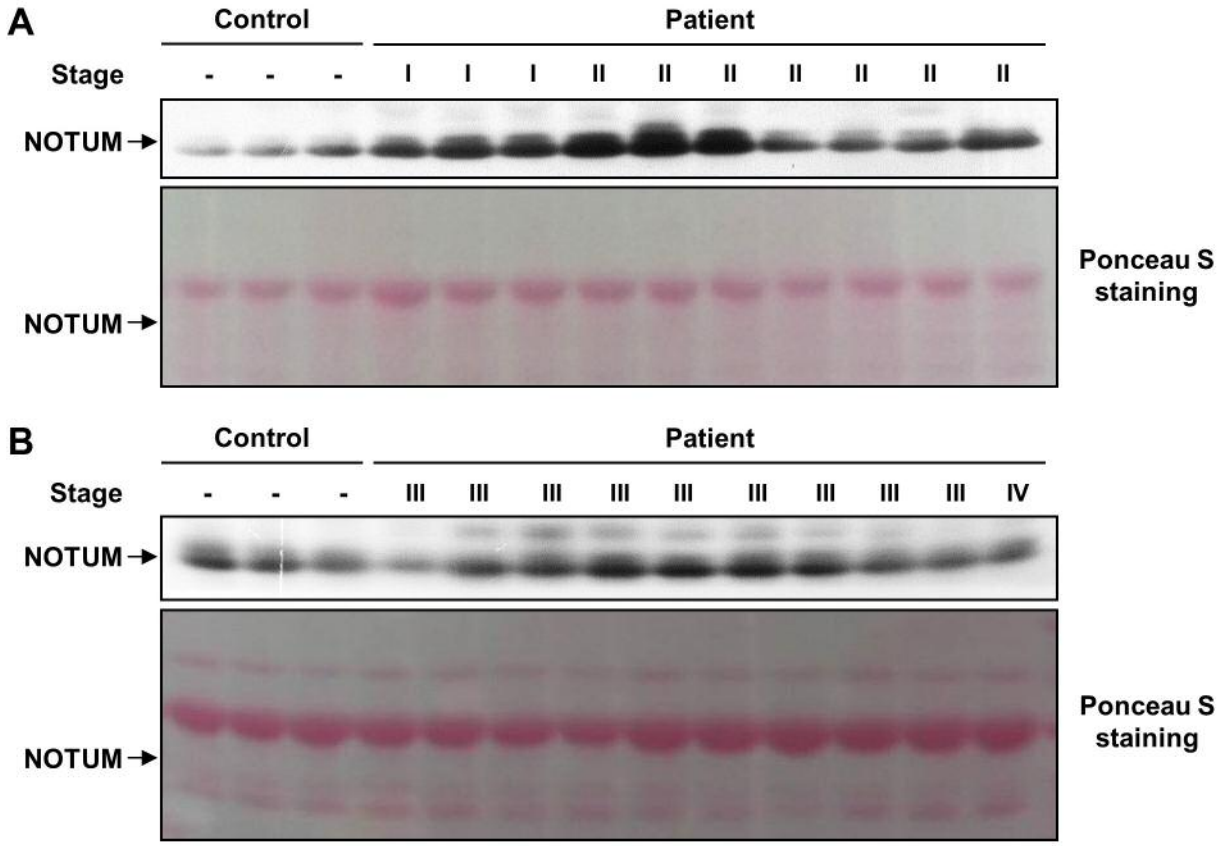

Figure 8. *Immunoblotting of palmitoleoyl-protein carboxylesterase (NOTUM) in plasma of healthy controls and patients with colorectal cancer (CRC). A: Healthy controls and patients with stage II CRC. B: Healthy controls and patients with stage II-IV CRC. Ponceau S-stained membranes are presented as protein loading controls.*

8 Kharaishvili G, Simkova D, Bouchalova K, Gachechiladze M, Narsia N and Bouchal J: The role of cancer-associated fibroblasts, solid stress and other microenvironmental factors in tumor progression and therapy resistance. Cancer Cell Int *14*: 41, 2014.

9 Hanahan D and Weinberg RA: Hallmarks of cancer: The next generation. Cell *144(5)*: 646-674, 2011.

10 Wels J, Kaplan RN, Rafii S and Lyden D: Migratory neighbors and distant invaders: Tumor-associated niche cells. Genes Dev *22(5)*: 559-574, 2008.

11 Xue H, Lu B, Zhang J, Wu M, Huang Q, Wu Q, Sheng H, Wu D, Hu J and Lai M: Identification of serum biomarkers for colorectal cancer metastasis using a differential secretome approach. J Proteome Res *9(1)*: 545-555, 2010.

12 de Wit M, Kant H, Piersma SR, Pham TV, Mongera S, van Berkel MP, Boven E, Ponten F, Meijer GA, Jimenez CR and Fijneman RJ: Colorectal cancer candidate biomarkers identified by tissue secretome proteome profiling. J Proteomics *99*: 26-39, 2014.

13 Ahmed D, Eide PW, Eilertsen IA, Danielsen SA, Eknaes M, Hektoen M, Lind GE and Lothe RA: Epigenetic and genetic features of 24 colon cancer cell lines. Oncogenesis *2*: e71, 2013.

14 Gagos S, Hopwood VL, Iliopoulos D, Kostakis A, Karayannakos P, Yatzides H, Skalkeas GD and Pathak S: Chromosomal markers associated with metastasis in two colon cancer cell lines established from the same patient. Anticancer Res *15(2)*: 369-378, 1995.

15 Ji H, Greening DW, Barnes TW, Lim JW, Tauro BJ, Rai A, Xu R, Adda C, Mathivanan S, Zhao W, Xue Y, Xu T, Zhu HJ and Simpson RJ: Proteome profiling of exosomes derived from human primary and metastatic colorectal cancer cells reveal differential expression of key metastatic factors and signal transduction components. Proteomics *13(10-11)*: 1672-1686, 2013.

16 Choi DS, Choi DY, Hong BS, Jang SC, Kim DK, Lee J, Kim YK, Kim KP and Gho YS: Quantitative proteomics of extracellular vesicles derived from human primary and metastatic colorectal cancer cells. J Extracell Vesicles 1, 2012. doi: 10.3402/jev.v1i0.18704

17 Elias JE and Gygi SP: Target-decoy search strategy for increased confidence in large-scale protein identifications by mass spectrometry. Nat Methods *4(3)*: 207-214, 2007.

18 Griffin NM, Yu J, Long F, Oh P, Shore S, Li Y, Koziol JA and Schnitzer JE: Label-free, normalized quantification of complex mass spectrometry data for proteomic analysis. Nat Biotechnol *28(1)*: 83-89, 2010.

19 Young GM, Radhakrishnan VM, Centuori SM, Gomes CJ and Martinez JD: Comparative analysis of 14-3-3 isoform expression and epigenetic alterations in colorectal cancer. BMC Cancer *15*: 826, 2015.

20 Yoon JH, Kim D, Jang JH, Ghim J, Park S, Song P, Kwon Y, Kim J, Hwang D, Bae YS, Suh PG, Berggren PO and Ryu SH: Proteomic analysis of the palmitate-induced myotube secretome reveals involvement of the annexin A1-formyl peptide receptor 2 (FPR2) pathway in insulin resistance. Mol Cell Proteomics *14(4)*: 882-892, 2015.

21 Yoon JH, Kim J, Kim KL, Kim DH, Jung SJ, Lee H, Ghim J, Kim D, Park JB, Ryu SH and Lee TG: Proteomic analysis of hypoxia-induced U373MG glioma secretome reveals novel hypoxia-dependent migration factors. Proteomics *14(12)*: 1494-1502, 2014.

22 Yoon JH, Song P, Jang JH, Kim DK, Choi S, Kim J, Ghim J, Kim D, Park S, Lee H, Kwak D, Yea K, Hwang D, Suh PG and Ryu SH: Proteomic analysis of tumor necrosis factor-alpha (TNF-alpha)-induced l6 myotube secretome reveals novel tnf-alpha-dependent myokines in diabetic skeletal muscle. J Proteome Res *10(12)*: 5315-5325, 2011.

23 Yoon JH, Yea K, Kim J, Choi YS, Park S, Lee H, Lee CS, Suh PG and Ryu SH: Comparative proteomic analysis of the insulin-induced l6 myotube secretome. Proteomics *9(1)*: 51-60, 2009.

24 Giraldez AJ, Copley RR and Cohen SM: HSPG modification by the secreted enzyme notum shapes the wingless morphogen gradient. Dev Cell *2(5)*: 667-676, 2002.

25 Traister A, Shi W and Filmus J: Mammalian NOTUM induces the release of glypicans and other GPI-anchored proteins from the cell surface. Biochem J *410(3)*: 503-511, 2008.

26 Zhang X, Cheong SM, Amado NG, Reis AH, MacDonald BT, Zebisch M, Jones EY, Abreu JG and He X: NOTUM is required for neural and head induction *via* wnt deacylation, oxidation, and inactivation. Dev Cell *32(6)*: 719-730, 2015.

27 Ayers KL, Gallet A, Staccini-Lavenant L and Therond PP: The long-range activity of hedgehog is regulated in the apical extracellular space by the glypican dally and the hydrolase notum. Dev Cell *18(4)*: 605-620, 2010.

28 Torisu Y, Watanabe A, Nonaka A, Midorikawa Y, Makuuchi M, Shimamura T, Sugimura H, Niida A, Akiyama T, Iwanari H, Kodama T, Zeniya M and Aburatani H: Human homolog of NOTUM, overexpressed in hepatocellular carcinoma, is regulated transcriptionally by beta-catenin/TCF. Cancer Sci *99(6)*: 1139-1146, 2008.

29 De Robertis M, Arigoni M, Loiacono L, Riccardo F, Calogero RA, Feodorova Y, Tashkova D, Belovejdov V, Sarafian V, Cavallo F and Signori E: Novel insights into NOTUM and glypicans regulation in colorectal cancer. Oncotarget *6(38)*: 41237-41257, 2015.

30 Fang JY and Richardson BC: The MAPK signalling pathways and colorectal cancer. Lancet Oncol *6(5)*: 322-327, 2005.

31 Wu WK, Wang XJ, Cheng AS, Luo MX, Ng SS, To KF, Chan FK, Cho CH, Sung JJ and Yu J: Dysregulation and crosstalk of cellular signaling pathways in colon carcinogenesis. Crit Rev Oncol Hematol *86(3)*: 251-277, 2013.

32 Velho S, Oliveira C, Ferreira A, Ferreira AC, Suriano G, Schwartz S Jr., Duval A, Carneiro F, Machado JC, Hamelin R and Seruca R: The prevalence of PIK3CA mutations in gastric and colon cancer. Eur J Cancer *41(11)*: 1649-1654, 2005.

33 Campbell IG, Russell SE, Choong DY, Montgomery KG, Ciavarella ML, Hooi CS, Cristiano BE, Pearson RB and Phillips WA: Mutation of the *PIK3CA* gene in ovarian and breast cancer. Cancer Res *64(21)*: 7678-7681, 2004.

34 Madan B, Ke Z, Lei ZD, Oliver FA, Oshima M, Lee MA, Rozen S and Virshup DM: NOTUM is a potential pharmacodynamic biomarker of WNT pathway inhibition. Oncotarget *7(11)*: 12386-12392, 2016.

35 Kuipers EJ, Grady WM, Lieberman D, Seufferlein T, Sung JJ, Boelens PG, van de Velde CJ and Watanabe T: Colorectal cancer. Nat Rev Dis Primers *1*: 15065, 2015.

36 Puccini A, Berger MD, Zhang W and Lenz HJ: What we know about c-JUN ii and iii colon cancer: It's still not enough. Target Oncol *12(3)*: 265-275, 2017.

37 Gao W and Ho M: The role of glypican-3 in regulating WNT in hepatocellular carcinomas. Cancer Rep *1(1)*: 14-19, 2011.

38 Kayed H, Kleeff J, Keleg S, Jiang X, Penzel R, Giese T, Zentgraf H, Buchler MW, Korc M and Friess H: Correlation of glypican-1 expression with TGF-beta, BMP, and activin receptors in pancreatic ductal adenocarcinoma. Int J Oncol *29(5)*: 1139-1148, 2006.
39 Hacker U, Nybakken K and Perrimon N: Heparan sulphate proteoglycans: The sweet side of development. Nat Rev Mol Cell Biol *6(7)*: 530-541, 2005.
40 Filmus J, Capurro M and Rast J: Glypicans. Genome Biol *9(5)*: 224, 2008.
41 Dreyfuss JL, Regatieri CV, Jarrouge TR, Cavalheiro RP, Sampaio LO and Nader HB: Heparan sulfate proteoglycans: Structure, protein interactions and cell signaling. An Acad Bras Cienc *81(3)*: 409-429, 2009.
42 Cassinelli G, Zaffaroni N and Lanzi C: The heparanase/heparan sulfate proteoglycan axis: A potential new therapeutic target in sarcomas. Cancer Lett *382(2)*: 245-254, 2016.
43 David CJ, Huang YH, Chen M, Su J, Zou Y, Bardeesy N, Iacobuzio-Donahue CA and Massague J: TGF-beta tumor suppression through a lethal emt. Cell *164(5)*: 1015-1030, 2016.
44 Li J, Ballim D, Rodriguez M, Cui R, Goding CR, Teng H and Prince S: The anti-proliferative function of the TGF-beta1 signaling pathway involves the repression of the oncogenic TBX2 by its homologue TBX3. J Biol Chem *289(51)*: 35633-35643, 2014.
45 Jahn SC, Law ME, Corsino PE and Law BK: TGF-beta antiproliferative effects in tumor suppression. Front Biosci *4*: 749-766, 2012.
46 Zhang YE: Non-smad pathways in tgf-beta signaling. Cell Res *19(1)*: 128-139, 2009.
47 Engel FB, Schebesta M, Duong MT, Lu G, Ren S, Madwed JB, Jiang H, Wang Y and Keating MT: P38 MAP kinase inhibition enables proliferation of adult mammalian cardiomyocytes. Genes Dev *19(10)*: 1175-1187, 2005.
48 Hui L, Bakiri L, Mairhorfer A, Schweifer N, Haslinger C, Kenner L, Komnenovic V, Scheuch H, Beug H and Wagner EF: P38alpha suppresses normal and cancer cell proliferation by antagonizing the JNK-c-JUN pathway. Nat Genet *39(6)*: 741-749, 2007.
49 Ventura JJ, Tenbaum S, Perdiguero E, Huth M, Guerra C, Barbacid M, Pasparakis M and Nebreda AR: P38alpha MAP kinase is essential in lung stem and progenitor cell proliferation and differentiation. Nat Genet *39(6)*: 750-758, 2007.
50 Hui L, Bakiri L, Stepniak E and Wagner EF: P38alpha: A suppressor of cell proliferation and tumorigenesis. Cell Cycle *6(20)*: 2429-2433, 2007.
51 Iyoda K, Sasaki Y, Horimoto M, Toyama T, Yakushijin T, Sakakibara M, Takehara T, Fujimoto J, Hori M, Wands JR and Hayashi N: Involvement of the p38 mitogen-activated protein kinase cascade in hepatocellular carcinoma. Cancer *97(12)*: 3017-3026, 2003.
52 Ventura JJ, Hubner A, Zhang C, Flavell RA, Shokat KM and Davis RJ: Chemical genetic analysis of the time course of signal transduction by JNK. Mol Cell *21(5)*: 701-710, 2006.
53 Deng Y, Ren X, Yang L, Lin Y and Wu X: A JNK-dependent pathway is required for TNFalpha-induced apoptosis. Cell *115(1)*: 61-70, 2003.
54 Edlund S, Bu S, Schuster N, Aspenstrom P, Heuchel R, Heldin NE, ten Dijke P, Heldin CH and Landstrom M: Transforming growth factor-beta1 (TGF-beta)-induced apoptosis of prostate cancer cells involves SMAD7-dependent activation of p38 by TGF-beta-activated kinase 1 and mitogen-activated protein kinase kinase 3. Mol Biol Cell *14(2)*: 529-544, 2003.
55 Huang DY, Chao Y, Tai MH, Yu YH and Lin WW: STI571 reduces trail-induced apoptosis in colon cancer cells: C-ABL activation by the death receptor leads to stress kinase-dependent cell death. J Biomed Sci *19*: 35, 2012.

Received July 24, 2018
Revised September 14, 2018
Accepted September 19, 2018